



Monitoring Vertical Land Movements in the Nile Delta, Egypt by GNSS Datasets Over 2012-2023

Gomaa M. Dawod*, Hoda F. Mohamed, Ahmed M. Amin

Survey Research Institute, National Water Research Center, Giza, Egypt

*Email: dawod_gomaa@yahoo.com

Abstract Vertical land movement is a natural and human hazard that should be precisely monitored. Global Navigation Satellite Navigation (GNSS), terrestrial levelling, and radar remote sensing provide various technical alternatives to monitor land subsidence. The current research has utilized 23 GNSS stations cover the period 2012-2023 to estimate precise rates of vertical land movements in the Nile delta region, Egypt. The Precise Point Positioning (PPP) approach of GNSS data processing has been utilized. An average accuracy of two millimeters has been accomplished using 24-hours continuous GNSS dataset at each station. The accomplished 3D findings demonstrate that the land vertical movements over the entire Nile delta region vary between -7.2 mm/year and +2.6 mm/year with an average equals -1.4 mm/year. Hence, it is recommended to take into account the influences of such hazardous phenomenon on the huge infrastructures and development plans in the Nile delta region that contains almost half of the population of Egypt.

Keywords GNSS, Land Subsidence, Uplift, PPP, Natural Hazards.

1. Introduction

The Nile delta region in Egypt, as a low-elevation coastal region, suffers from several environmental natural hazards affecting the population and the economy. Some of these global climate-change based hazards include, among others, Sea Level Rise (SLR), land subsidence, sea-water intrusion [1], soil degradation [2], SLR inundation [3], and coastline retreat [4]. The vertical land movements comprise a vital hazard depends on natural and human causes. Vertical land movements, particularly land subsidence, defined as the settlement of the land surface resulted from human-induced and natural-driven processes. Land subsidence could be attributed to natural compaction of unconsolidated deposits, groundwater extraction for examples. A recent study highlighted that nineteen percent of the global population face a high probability of subsidence [5]. On another scene, land subsidence could be dangerous and reach as high as 44 mm/year in some regions worldwide [6].

Several approaches have been carried out to monitor subsidence particularly in the Nile delta region. Gebremichael et al. [7] have utilized radar interferometric approach over 2004 to 2010 to monitor land subsidence over the entire Nile delta of Egypt. Their results showed that land subsidence could be as -9.7 mm/year over the north central and northeastern delta where uplift of 2.5 mm/year occurred that separates the highly subsiding northern block from the stable or slightly uplifting southern delta block. Moreover, Becker and Sultan [8] utilized radar remote sensing images over 1992-1999 and showed that land subsidence could be as much as -8 mm/year over the Nile delta region. Land subsidence could be also estimated from tide gauges and satellite altimetry measurements [9]. Traditionally, land subsidence have been monitored by precise levelling [10]. More recently, the Global Navigation Satellite Systems (GNSS) have been utilized to precisely estimate land subsidence [11]. AbouAly et al. [12] have utilized 8 GNSS stations through 2013-2015 to estimate land subsidence over the Nile delta. Their results showed that the highest subsidence rate is found at Mansoura and



Port Said city where it ranges between 2.5 mm/year to 10 mm/year. The Precise Point Positioning (PPP) is considered one of the most precise GNSS data processing alternative to ensure high precision in land subsidence and crustal deformation [13].

The current research employed the PPP approach for processing GNSS datasets over 2012-2023 to estimate recent rates of vertical land movements in the Nile delta.

2. Study Area and Available Data

The study area in the current research not only limited by the classical definition of the Nile delta as bounded by the two branches of the Nile River. It is extended in the west direction to include the Alexandria city and in the east direction to include the Suez Canal too. Accordingly, it extends from longitude 29.8° E to 32.4° E and from latitude 29.9° N to 31.6° N covers 34785.6 km² as depicted in Fig. 1.

23 GNSS stations have been acquired from the Egyptian Survey Authority (ESA) over the study area (Fig. 1). A set of several observation files for each station covering continuous 24-hour session have been collected annually from 2012 to 2023. Few observation files have been missing at some stations due to communication problems between the stations and the GNSS data center at ESA headquarter. The collected GNSS datasets are tabulated in Appendix 1.

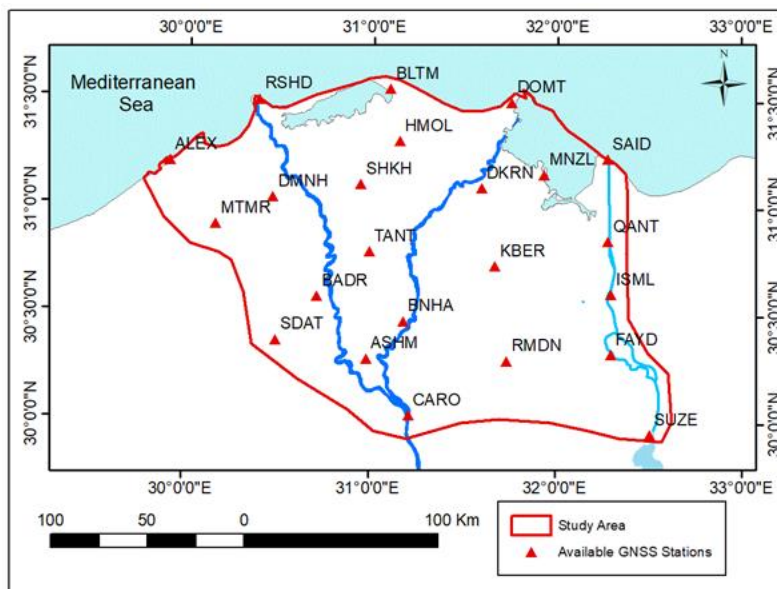


Figure 1: Study Area and Available GNSS Stations

3. Methodology

First, the PPP approach of the GNSS data processing has been carried out several times at each stations for all available observation sessions. PPP modeling relates the ionosphere-free combinations of dual-frequency GPS pseudorange (P_i , $i = 1, 2$) and carrier phase observations (ϕ_i) to the unknown parameters according to the following simplified observation equations [14]:

$$l_p = \rho(X_s, X_r) + c(dT - dt) + T_r + \varepsilon_p \quad (1)$$

$$l_\phi = \rho(X_s, X_r) + c(dT - dt) + T_r + N\lambda + \varepsilon_\phi \quad (2)$$

where,

l_p is the ionospheric-free combination of P_1 and P_2 pseudoranges,

l_ϕ is the ionospheric-free combination of ϕ_1 and ϕ_2 carrier phases,

N is the non-integer ambiguity,

X_s is the satellite Cartesian coordinates at transmission time,

X_r is the GPS Cartesian coordinates at reception time,

dT is the GPS receiver clock offset from the GPS time,

dt denotes the satellite clock offset from the GPS time,



T_r is the signal path delay to the neutral-atmospheric (mainly troposphere),
 λ is the wavelength, and
 ε denotes the noises.

The Trimble Business Center (TBC) version 5.2 software has been utilized to perform the PPP computations. The satellite precise orbits and clock corrections have been downloaded from the International GNSS Service (IGS) website: <https://igs.org/>. Consequently, a time series of ellipsoidal elevations has been obtained, relative to International Terrestrial Reference Frame 2014 (ITF2014) for each station over its corresponding available time span.

Next, a first-order regression is fitted for the elevations of each station to model its vertical movements in the form of:

$$h = a_0 + a_1 \text{Year} \quad (3)$$

where, a_0 and a_1 are unknowns to be determined and Year represents the observation time in years. The unknown a_1 represents the annual vertical movement at such a station.

The coefficient of determination, R^2 , is computed to describe the goodness of the regression as:

$$R^2 = 1 - \frac{\sum (h_i - h_p)^2}{\sum (h_i - h_m)^2} \quad (4)$$

where,

h_i is the i^{th} observed elevation of the current station,

h_p is the i^{th} predicted elevation observation of the current station,

h_m is the i^{th} mean elevation observation of the current station,

Statistically speaking, R^2 represents the goodness of fit of a regression model. It ranges from 0 to 1, and as it goes to 1 indicates the strength of the model. If its value is less than 0.5, the attained regression model might not be trustable.

Collecting all trustable regression trends of vertical land movements at available GNSS stations, the Arc GIS 10.8 software is utilized to build a 3D model of land movement phenomena over the study area. The processing steps are depicted in Fig. 2.

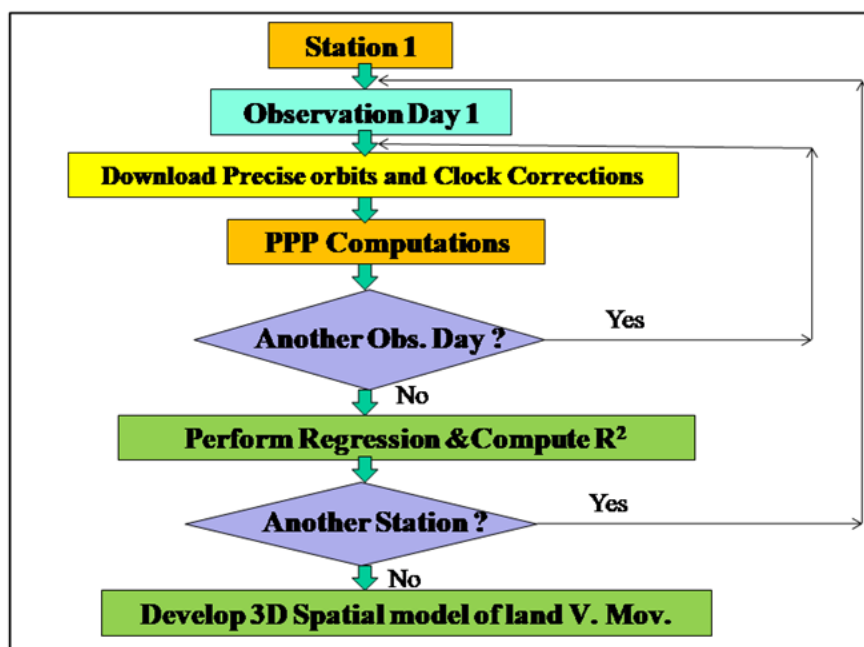


Figure 2: Flowchart of the Processing Steps

4. Processing and Results

Investigating the results of PPP GNSS processing showed that the attained elevation typical accuracy range from ± 0.002 to ± 0.006 m with an average equals ± 0.003 m (Fig. 3). Such an accuracy level was expected since



the utilized GNSS sessions comprise 24-hour continuous datasets. Next, the findings of the regression modelling indicate that 15 out of the utilized GNSS stations have a good-fit regression models with R^2 values greater than 0.5. Fig. 4 depicts a typical example of such a situation at Port Said station. Such stations along with their statistics are depicted in Fig. 5 and tabulated in Table 1. The remaining stations, with weak R^2 values, might be an indication that the vertical land movements phenomenon do not possess a linear regression model over 2012-2023 and more GNSS data are required. From Table 1, it can be realized that the vertical land movements in the Nile delta region consists generally from subsidence ranges between -0.0005 m at MTMR station and -0.005 m at both SAID and TANT stations. Few GNSS stations showed uplift varying between $+0.001$ at Suez and $+0.002$ m at BADR [15]. It worth mentioning that the accomplished findings generally agree with results of similar research studies at the Nile delta region.

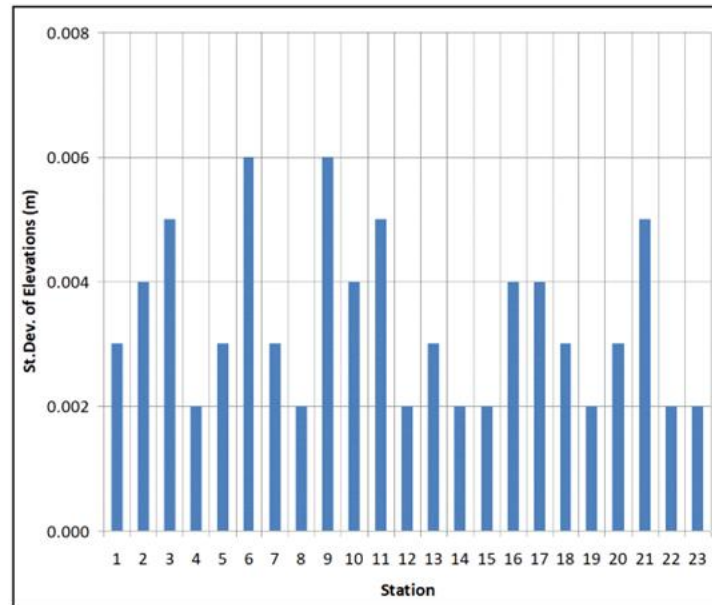


Figure 3: Typical Accuracy of Accomplished GNSS Elevations

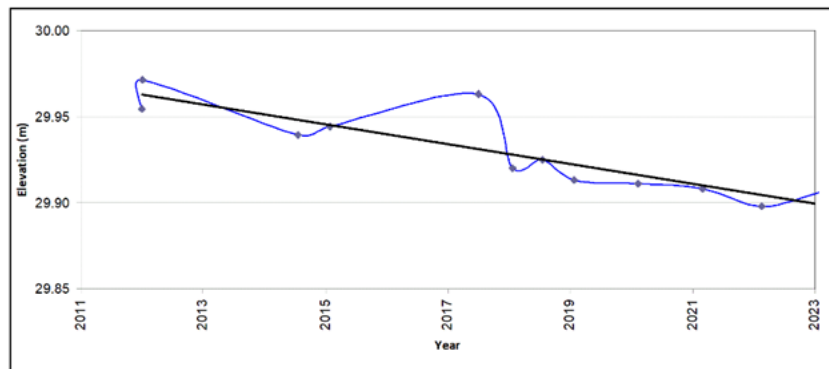


Figure 4: A Typical Example of Linear Regression at Port Said GNSS Station



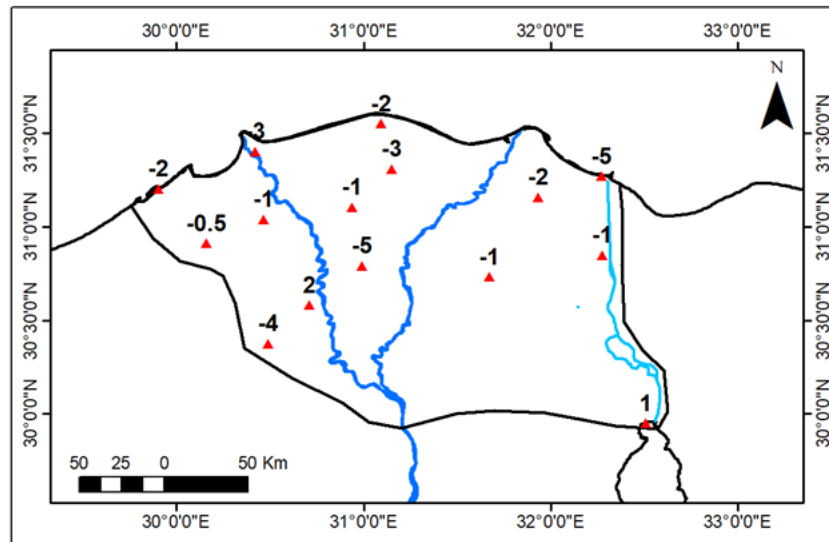


Figure 5: Rates of Vertical Land Movements at GNSS Stations

Table 1: Statistics of Linear Regression at GNSS Stations

Station	Regression	Annual Trend (mm/year)	R2
BLTM	$h = -0.002 \text{ year} + 36.11$	-2	0.93
SKKH	$h = -0.001 \text{ year} + 34.09$	-1	0.82
BADR	$h = 0.002 \text{ year} + 43.98$	+2	0.81
MNZL	$h = -0.002 \text{ year} + 41.57$	-2	0.78
DMNH	$h = -0.001 \text{ year} + 45.25$	-1	0.77
SAID	$h = -0.005 \text{ year} + 41.51$	-5	0.77
RSHD	$h = -0.003 \text{ year} + 44.83$	-3	0.73
TANT	$h = -0.005 \text{ year} + 51.38$	-5	0.71
ALEX	$h = -0.002 \text{ year} + 72.09$	-2	0.71
KBER	$h = -0.001 \text{ year} + 35.57$	-1	0.68
HMOL	$h = -0.003 \text{ year} + 50.14$	-3	0.67
SUEZ	$h = 0.001 \text{ year} + 44.31$	+1	0.55
SDAT	$h = -0.004 \text{ year} + 81.42$	-4	0.54
MTMR	$h = -0.0005 \text{ year} + 34.1616$	-0.5	0.54
QANT	$h = -0.001 \text{ year} + 36.33$	-1	0.53

Finally, the GIS-based analysis tools have been performed to convert the vertical land movements rates at discrete GNSS points to a 3D spatial model (Fig. 6). Accordingly, the land vertical movements over the entire Nile delta region found to range from -7.2 mm/year and 2.6 mm/year with an average equals -1.4 mm/year. Fig. 6 shows also that the higher subsidence occurred at the most northeast of the study area at Port Said city and the central west area around Tanta city. Additionally, the uplift occurs in the eastern area around Suez city and around Badr city too. Furthermore, the vertical land movement phenomenon has been investigated over the governorates (administration units) in the study area. Fig. 7 and Table 2 present the accomplished findings. Thus, it can be recognized that Gharbiya, Daqahlia, and Port Said governorates have the higher rates of annual land subsidence. Thus, it is recommended to pay attention to the effects of land subsidence mainly in the operation and management planes of huge infrastructures in such regions.



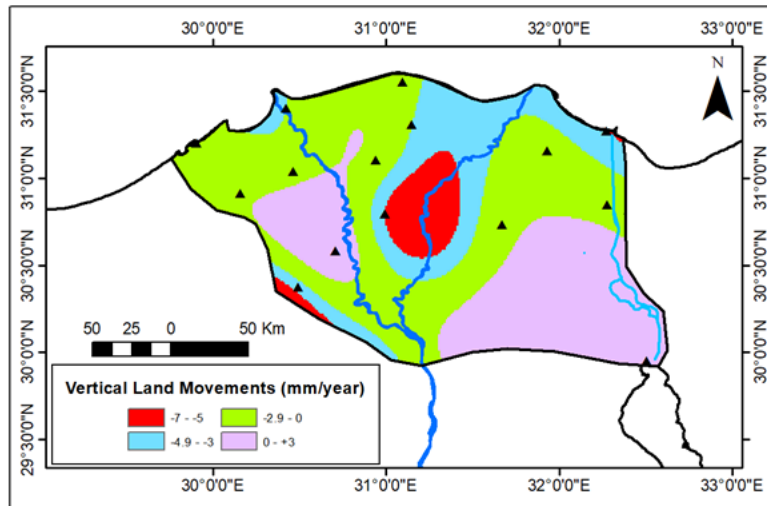


Figure 6: 3D Model of Vertical Land Movements in The Nile Delta Region

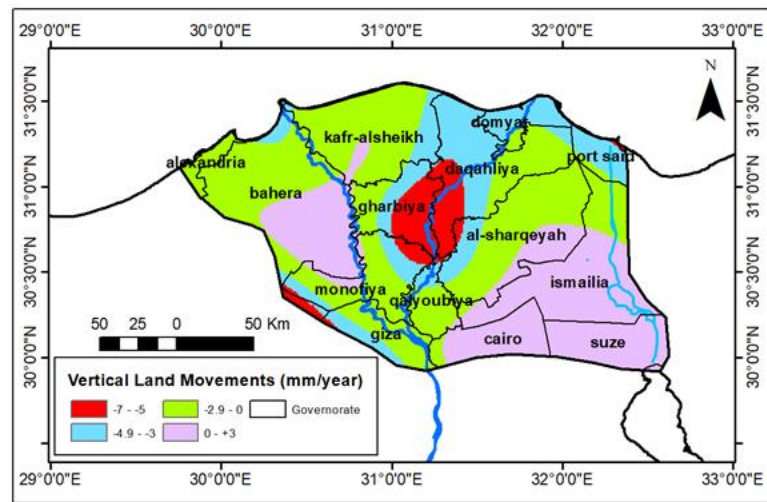


Figure 7: Vertical Land Movements in The Nile Delta Governorates

Table 2: Statistics of Vertical Land Movements in The Nile Delta Governorates (mm/year)

Governorate	Min	Max	Mean
Gharbiya	-5.98	0.97	-4.32
Daqahlia	-7.15	-1.39	-3.92
Port Said	-5.21	-2.55	-3.69
Damietta	-4.25	-2.39	-3.42
Menofia	-7.16	1.06	-2.47
Giza	-5.88	-0.62	-2.43
Qalioubiya	-5.68	0.31	-1.984
Alexandria	-2.9	-1.39	-1.94
Kafr El-Sheikh	-4.93	0.17	-1.49
Sharqiya	-5.99	0.77	-1.21
Beherra	-5.41	2.55	-0.4
Ismalia	-2.95	1.66	0.48
Suez	0.13	2.11	1.29
Cairo	-0.96	2.38	1.4

5. Conclusions

The PPP approach of GNSS comprise an effective and cost-effective technical method for monitoring vertical land movements over a region. Based on GNSS datasets at 23 stations over the 2012-2023 period, the current study aims to precisely monitor the vertical land movement phenomena in the Nile delta region, Egypt. It has been found that 15 stations showed trustable land movement trends while the remaining stations do not, which implicitly recommend that more GNSS data are required over longer period of times.

Land subsidence is an ongoing natural and human phenomenon in the Nile delta region. Based on the results of 23 GNSS, it has been shown that several locations in the study area have experienced land subsidence, with an average rate of about -1.4 mm/year and can go up to about -5 mm/year in certain locations. Moreover, some regions in that area showed relatively minor uplift of almost 2 mm/year.

Causes of land subsidence, such as groundwater extraction and urban development, need to be investigated in details. Effects of land subsidence to the absolute estimation of sea level rise should be studied too. Additionally, it has been recognized that Gharbiya, Daqahlia, and Port Said governorates have the higher rates of annual land subsidence. Thus, it is recommended to take into consideration such effects in the operation and management plans of huge infrastructures in such regions.

Conflicts of interest statement: The authors declare that there is no conflicts of interest.

Funding information: No fund was allocated to the current research study.

References

- [1]. Abdelfattah, M., Abu-Bakrm H., Aretouyap, Z., Sheta, M., Hassan, T., Geriesh, M., Shaheen, S., Alogayell, H., EL-Bana, E., and Gaber, A. (2023) Mapping the impacts of the anthropogenic activities and seawater intrusion on the shallow coastal aquifer of Port Said, Egypt, *Frontiers in Earth Science*, 11:1204742. <https://doi.org/10.3389/feart.2023.1204742>
- [2]. Abowaly, M., Ali, R., Moghanm, F., Gharib, M., Moustapha, M., Elbagory, M., Omara, A., and Elmahdy, S., (2022) Assessment of soil degradation and hazards of some heavy metals, using Remote Sensing and GIS techniques in the Northern part of the Nile Delta, Egypt, *Agriculture*, <https://doi.org/10.3390/agriculture13010076>
- [3]. El-Quilish, M., El-Ashquer, M., Dawod, G. and El Fiky, G. (2023) Development of an Inundation Model for the Northern Coastal Zone of the Nile Delta Region, Egypt Using High-Resolution DEM, *Arabian Journal for Science and Engineering*, 48:601–614, <https://doi.org/10.1007/s13369-022-07013-y>
- [4]. El-Asmar, H. and Al-Olayan, H. (2013) Environmental Impact Assessment and Change Detection of the Coastal Desert along the Central Nile Delta Coast, Egypt, *International Journal of Remote Sensing Applications*, V. 3, No. 3, pp. 159-170.
- [5]. Herrera-Garcia, G., Ezquerro, P., Tomás, R., Béjar-Pizarro, M., López-Vinielles, J., Rossi, M., Mateos, R., Carreón-Freyre, D., Lambert, J., Teatini, P., Cabral-Cano, E., Erkens, G., Galloway, D., Hung, W., Kakar, N., Sneed, M., Tosi, L., Wang, H., and Ye, S. (2021) Mapping the global threat of land subsidence, *Insights*, <https://doi.org/10.1126/science.abb8549>.
- [6]. Karlsrud, K., Tunbridge, L., Khanh, N. and Dinh, N. (2020) Preliminary results of land subsidence monitoring in the Ca Mau Province, *Proc. IAHS*, No. 382, pp. 111–115.
- [7]. Gebremichael, W., Sultan, M., Becker, R., El Bastawesy, M., Cherif, O. and Emil, M. (2018) Assessing Land Deformation and Sea Encroachment in the Nile Delta: A Radar Interferometric and Inundation Modeling Approach, *Journal of Geophysical Research: Solid Earth*, 123, 3208–3224, <https://doi.org/10.1002/%202017JB015084>
- [8]. Becker, R. and Sultan, M. (2009) Land subsidence in the Nile Delta: inferences from radar interferometry, *The Holocene*, V. 19, No. 6, pp. 949–954.
- [9]. Braitenberg, C., Mariani, P., Tunini, L., Grillo, B. and Nagy, I. (2010) Vertical crustal motions from differential tide gauge observations and satellite altimetry in southern Italy, *Journal of Geodynamics*, <https://doi.org/10.1016/j.jog.2010.09.003>



[10]. Fisher, B. and Minkel, D. (2009) Evaluation of Survey Control Stations Height Stability in Subsidence Zone, Available from: <https://content.civicplus.com/api/assets/12cd72e5-aba7-45e8-974b-5fa181530efb>, Accessed Sept. 12, 2023 .

[11]. Facio, Y. and Berber, M. (2019) Subsidence is determined in the heart of the Central Valley using Post Processed Static and Precise Point Positioning techniques, Applied Geodesy, <https://doi.org/10.1515/jag-2019-0043>.

[12]. AbouAly, N., Hussien, M., Rabah, M., Zidan, Z. and Saleh, M. (2021a) Land deformation monitoring by GNSS in the Nile Delta and the measurements analysis, Arabian Journal of Geosciences,14:150, <https://doi.org/10.1007/s12517-021-06497-6>

[13]. AbouAly, N., Hussien, M., Rabah, M., and Zidan, Z. (2021b) Assessment of NRCAN PPP online service in determination of crustal velocity: case study Northern Egypt GNSS Network, Arabian Journal of Geosciences, 14:188, <https://doi.org/10.1007/s12517-021-06530-8>.

[14]. Ayhan, M. and Almuslmani, B. (2021) Positional accuracy and convergence time assessment of GPS precise point positioning in static mode, Arabian Journal of Geosciences, 14: 1263, <https://doi.org/10.1007/s12517-021-07428-1>.

[15]. SRI (Survey Research Institute) (2023) Assessing and modelling of land subsidence in the Nile delta area over 2012 – 2023, A technical report in Arabic, Giza, Egypt.

Appendix 1: Available GNSS Stations

St. No.	Year/St.	1	2	3	4	5	6	7	8	9	10	11	12	13	14	15	16	17	18	19	20	21	22	23
	ALEX																							
	ASHM																							
	BADR																							
	BLTM																							
	BNHA																							
	CARO																							
	DKRN																							
	DMNH																							
	DOMT																							
	FAYD																							
	HMOL																							
	ISML																							
	KBER																							
	MNZL																							
	MTMR																							
	QANT																							
	RMDN																							
	RSHD																							
	SAID																							
	SDAT																							
	SHKH																							
	SUEZ																							
	TANT																							

